Liquid Crystals

Publication details, including instructions for authors and subscription information:
http://www.informaworld.com/smpp/title~content=t713926090

New series of ferroelectric liquid crystals with two or three chiral centres exhibiting antiferroelectric and hexatic phases

M. Kapar; V. Hamplová; V. Novotná; M. Glogarová; D. Pociecha; P. Vank

To cite this Article Kapar, M. , Hamplová, V. , Novotná, V. , Glogarová, M. , Pociecha, D. and Vank, P.(2001) 'New series of ferroelectric liquid crystals with two or three chiral centres exhibiting antiferroelectric and hexatic phases', Liquid Crystals, 28: 8, 1203 — 1209

To link to this Article: DOI: 10.1080/02678290110051602

URL: http://dx.doi.org/10.1080/02678290110051602

LIQUID CRYSTALS, 2001, VOL. 28, NO. 8, 1203–1209

New series of ferroelectric liquid crystals with two or three chiral centres exhibiting antiferroelectric and hexatic phases

M. KAŠPAR, V. HAMPLOVÁ, V. NOVOTNÁ, M. GLOGAROVÁ*,
D. POCIECHA† and P. VANĚK

Institute of Physics, Academy of Sciences of the Czech Republic, Na Slovance 2,
182 21 Prague 8, Czech Republic
†Laboratory of Dielectrics and Magnetics, Chemistry Department,
Warsaw University, Al. Zwirki i Wigury 101, 02-089 Warsaw, Poland

(*Received 25 November 2000; in final form 1 February 2001; accepted 13 February 2001*)

New series of liquid crystals with a chiral chain containing two asymmetric carbon atoms in two lactate groups have been synthesized. Some compounds have a third asymmetric centre in an (*S*)-2-methylbutyl alkyl chain. All the new compounds have SmA, SmC* and hexatic phases. Two of the homologues with three chiral centres also exhibit very wide SmC$_A$ phases and one of them a re-entrant SmC* phase. The phases are characterized by DSC, dielectric, and X-ray studies. Spontaneous polarization and tilt angle are determined for the polar phases.

1. Introduction

General structures for the compounds studied and denoted as ZLL *n*/*m* and ZLL *n*/* are, respectively

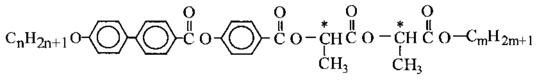

and

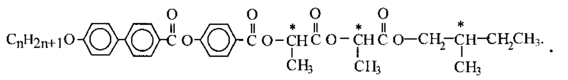

Recently a series of compounds of similar structure having only one chiral centre in a lactate unit was studied [1] and shown to exhibit wide ferroelectric (FE) SmC* and SmA phase ranges. No antiferroelectric (AF) phase was found in this series. The only similar compound with two chiral centres in lactate units was studied by Mery and co-workers [2], but that material had the chiral part connected to the core by the ether linkage. Its phase sequence was Cr 88.8 (SmC$_A^*$ 47.0 SmC$_\gamma^*$ 50.6 SmC* 70.0) SmA 105.5 I (°C), the phases in parenthesis being monotropic. The configuration of the two chiral centres was opposite (*R*, *S*), and one of the alkyl chains was very short.

With the aim of obtaining a wide temperature range AF material we have synthesized new series with longer alkyl chains or compounds with three chiral centres connected to the core by the ester group. All asymmetric centres have the (*S*) configuration. Mesomorphic properties and basic characteristics of the new compounds have been determined.

2. Synthesis

General scheme of synthesis:

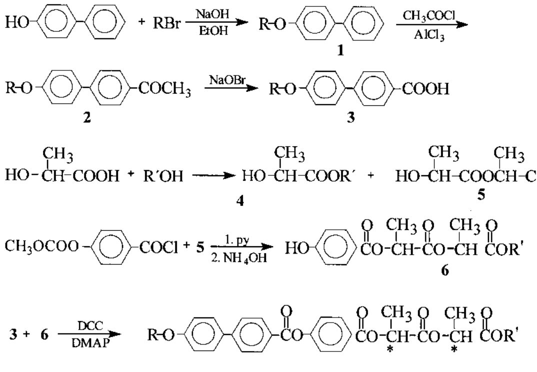

2.1. *Synthesis of 4-alkoxybiphenyl-4′-carboxylic acids (3)*

The synthesis was carried out according to a modified procedure [3] without involving demethylation, which usually decreases the yield. 4-Hydroxybiphenyl was converted into the ether (**1**). A solution of 0.4 mol of (**1**) and 53 g of anhydrous AlCl$_3$ in 0.5 l of 1,2-dichloroethane was cooled in an ice bath and 31 g of acetyl chloride was added drop-wise. The mixture was stirred for 2 h under cooling and another 2 h at room temperature and then treated with ice and HCl. The solvent was distilled off and the solid was dissolved in 0.5 l of boiling ether.

---

*Author for correspondence; e-mail: glogarova@fzu.cz

Liquid Crystals ISSN 0267-8292 print/ISSN 1366-5855 online © 2001 Taylor & Francis Ltd
http://www.tandf.co.uk/journals
DOI: 10.1080/02678290110051602

The desired *para*-product crystallized in the refrigerator (the *ortho*-isomer is more soluble). After recrystallization from diethyl ether, the pure white solid (**2**) was obtained.

NMR for compound (**2**) in $CDCl_3$, $R = C_8H_{17}$: 8.0 d (2 HAr *ortho* to $-COCH_3$); 7.64 and 7.58 dd (4HAr); 7.0 d (2 HAr *ortho* to RO−); 4.0 t (2H, $-CH_2O-$); 2.64 s (3H, CH_3CO-); 1.2–1.7 m (12H, CH_2); 0.90 t (3H, CH_3).

A solution of NaOBr prepared from 84 g NaOH and 30 ml of bromine was added in 6 portions during 1 h to a stirred mixture of 43 g of (**2**) in 200 ml of dioxane. After 2 h the suspension of the sparingly soluble sodium salt was treated with an excess of sodium bisulphite. One litre of water was added, the suspension was filtered and the filtercake washed twice with 50 ml of $CHCl_3$, 50 ml of cold dioxane and a 10% solution of HCl. A single crystallization from chloroform gave pure 4-alkoxybiphenyl-4′-carboxylic acid (**3**).

NMR for compound (**3**) in DMSO, $R = C_8H_{17}$: 7.95 d (2HAr *ortho* to −COOH); 7.6–7.8 m (4HAr); 7.0 d (2HAr *ortho* to RO−); 3.98 t (2H, CH_2O-); 1.7 quint. (2H, $\underline{CH_2}CH_2O$); 1.2–1.5 m (10H, CH_2); 0.82 t (3H, CH_3).

2.2. *Synthesis of α-(S)-(alkyloxycarbonyl)ethyl (S)-lactates (5)*

A solution of L-lactic acid (80% solution, 120 g) and 1 mol of the appropriate alcohol in 300 ml of benzene was heated in a Dean–Stark trap for 10 h. Benzene was evaporated off and the residue filtered and distilled in vacuum; the first fraction was the alcohol, the second was the corresponding alkyl (*S*)-lactate (**4**), and the third was the lactate (**5**).

NMR for compound (**5**) in $CDCl_3$, $R' = C_6H_{13}$: 5.15 q (1H, $\underline{CH}COOR'$); 4.35 q (1H, $\underline{CH}-OH$); 4.1 m (2H, $COOCH_2$); 1.48 and 1.52 dd (6H, $\underline{CH_3}CH$); 1.2–1.7 m (8H, CH_2); 0.88 t (3H, CH_3).

The boiling points, yields and optical activities for lactates are shown in table 1.

2.3. *Synthesis of compounds (6)*

The compounds (**6**) were prepared in a similar way to the *n*-alkyl (*S*)-2-(4-hydroxybenzoyloxy)propanoates described in our previous work [4]. Boiling points for the compounds (**6**) with *n*-hexyl and (*S*)-2-methylbutyl chains are 235°C/0.8 torr and 220°C/2 torr, respectively.

NMR for compound (**6a**) in $CDCl_3$, $R' = C_6H_{13}$: 7.9 d (2HAr *ortho* to −COOH); 6.8 d (2HAr, *ortho* to −OH); 5.3 q (1H, $ArCOO\underline{C}H$); 5.15 q (1H, $\underline{CH}COOR'$); 4.1 m (2H, $-COO\underline{CH_2}-$); 1.65 d (3H, $\underline{CH_3}-CH$) 1.5 d (3H, $\underline{CH_3}CHCOOR'$); 0.9 t (3H, CH_3). NMR for compound (**6b**) in $CDCl_3$, $R' = CH_2CH\ (CH_3)-CH_2-CH_3$: 7.9 d (2HAr); 6.8 d (2HAr); 5.35 q (1H, $ArCOO\underline{CH}$); 5.2 q (1H, $\underline{CH}COOR'$), 4.0 m (2H, $-COO\underline{CH_2}$); 1.6 and 1.4 and 1.2 m (1H + 1H + 1H, $-CH-CH_2-$); 0.9 m (6H, CH_3).

2.4. *Synthesis of final product (7)*

N,*N*′-dicyclohexylcarbodiimide (15 mmol) was added with stirring to a solution of 10 mmol of phenol (**6**) and 10 mmol of mesogenic acid (**3**) in 100 ml of dichloromethane. Stirring was continued for 12 h at room temperature. The crude product was chromatographed on silica gel (Kieselgel 60, Merck, Darmstadt) using a mixture of dichloromethane and acetone (98 : 2) as eluent. After crystallization from ethanol the product purity was determined by HPLC which was carried out with an Ecom high performance liquid chromatograph using the silica gel column Separon 7 μm, 3 × 150, Tessek with a mixture of toluene and methanol as eluent. The structures of all compounds were confirmed by ^1H NMR.

NMR for compound (**7**) in $CDCl_3$, $R = C_8H_{17}$; $R' = C_6H_{13}$: 8.2 dd (4HAr, *ortho* to −COO); 7.7 and 7.6 dd (4HAr); 7.34 d (2HAr *ortho* to ArCOO−); 7.0 d (2HAr *ortho* to RO−); 5.4 q and 5.2 q (1H + 1H, CH); 4.16 t (2H, $-COO-\underline{CH_2}-$); 4.02 t (2H, $\underline{CH_2}OAr$); 1.55 and 1.70 dd (3H + 3H, $\underline{CH_3}CH^*$); 1.2–1.9 m (10H, CH_2); 0.90 m (6H, CH_3).

3. Experimental results

All materials synthesized were studied by DSC (Perkin–Elmer 7) with cooling and heating rates of 5 K min^{-1}. The samples were (5–14 mg) placed in a nitrogen atmosphere and hermetically sealed in aluminium pans. Microscopic observations and measurement of basic characteristics were carried out using planar cells 25 μm thick filled in the isotropic phase. The cells were composed of glass plates provided with transparent ITO electrodes and polyimide layers rubbed in the same direction, thus ensuring a planar (bookshelf) geometry.

Table 1. The boiling points, yields and optical activities for lactates **4** and **5**.

	B.p./°C		$[\alpha]_D^{20}$ neat/°		Yield/%	
R′	**4**	**5**	**4**	**5**	**4**	**5**
n-Hexyl	78/2 torr	116/1 torr	− 11.8	− 27.4	56.0	10.4
(*S*)-2-Methylbutyl	53/2 torr	110/2 torr	− 11.1	− 47.5	60.7	14.7

Samples were aligned by applying an a.c. electric field (typically 5×10^6 V m^{-1}, 20 Hz). Temperature was controlled and stabilized with an accuracy of ± 0.1°C in a hot stage (Linkam). X-ray studies were performed using a DRON system equipped with a Ge monochromator. All X-ray experiments were conducted in the reflection mode for homeotropically aligned samples with one surface left free. The helix pitch was measured by light diffraction from non-aligned planar samples, and the optical rotatory power using free standing films.

3.1. *Mesomorphic properties*

The phase transition temperatures and enthalpies were evaluated by DSC (table 2). Typical DSC plots are shown in figures 1 (*a*) and 1 (*b*), in (*b*) the phase transitions with very low enthalpy being magnified. One can distinguish between the form of the non-symmetrical transition peaks for the second order SmA–SmC* transition and the symmetrical peaks, which correspond to the first order transitions between other mesophases, see figure 1 (*b*). We also mention the transition peaks to the hexatic phase with characteristic broad wings on both sides, which is a consequence of pre-transitional thermal fluctuations [5]. Phase types were determined from observations of textures and texture changes. All materials studied exhibit SmA, SmC*, and hexatic, phases. The AF $\mathrm{SmC}^*_{\mathrm{A}}$ phase was found for ZLL7/* and ZLL8/* only. The existence of the AF and hexatic phases was confirmed by our dielectric and X-ray studies, respectively (see below).

In ZLL7/* a re-entrant SmC* phase, $\mathrm{SmC}^*_{\mathrm{re}}$, occurs between the $\mathrm{SmC}^*_{\mathrm{A}}$ and hexatic phases. Its texture is the same as that of the high temperature SmC* phase. Both differ significantly from the $\mathrm{SmC}^*_{\mathrm{A}}$ phase, particularly in the density of the dechiralization lines, which reflects the helical pitch length. The pitch length is about 1 µm in the upper SmC* phase; it jumps up at the upper limit of the $\mathrm{SmC}^*_{\mathrm{A}}$ phase and then critically increases on cooling. Near the phase transition to the $\mathrm{SmC}^*_{\mathrm{re}}$ phase, the helix becomes unwound. Below the transition to the $\mathrm{SmC}^*_{\mathrm{re}}$, phase the helix is restored with the opposite handedness. The helix inversion was confirmed by the inversion of the sign of the optical rotatory power.

When mixtures of the ZLL7/* and ZLL6/* homologues are examined, a pocket of the $\mathrm{SmC}^*_{\mathrm{A}}$ phase surrounded by the SmC* phase is seen in the phase diagram, ending at a concentration of about 60% of ZLL7/*. For lower concentrations only the SmC* phase exists. In some compounds a low temperature crystalline phase occurs and is denoted as CrX, which is probably the CrG* or CrJ* phase. The texture in this phase exhibits some dechiralization lines, indicating a tilted structure with a space modulation.

Table 2. Transition temperatures between phases (°C) and transition enthalpies (J g^{-1} in square brackets); ● the phase exists, − the phase does not exist.

Compound	M.p.[a]	Cr		CrX		hex		$\mathrm{SmC}^*_{\mathrm{re}}$		$\mathrm{SmC}^*_{\mathrm{A}}$		SmC*		SmA		I
ZLL 6/*		●	< 20	●	65.5 [− 4.9]	●	76 [− 2.9]	—		—		●	97 [− 0.06]	●	141 [− 8.1]	●
ZLL 7/*	60.5 [17.6]	●	54 [− 12.3]	—		●	65 [− 2.2]	●	71 [− 0.06]	●	98 [− 0.04]	●	104 [− 0.19]	●	129 [− 5.7]	●
ZLL 8/*	68 [27.9]	●	48 [− 14.9]	—		●	58[b] [− 1.5]	—		●	99 [− 0.07]	●	102 [− 0.21]	●	126 [− 5.0]	●
ZLL 6/6		●	< 20	●	62.5 [− 4.6]	●	72 [− 2.7]	—		—		●	80 [− 0.04]	●	135 [− 7.3]	●
ZLL 7/6	57 [19.0]	●	49.5 [− 14.1]	—		●	59 [− 2.4]	—		—		●	88 [− 0.11]	●	126 [− 5.4]	●
ZLL 8/6	57 [22.8]	●	47 [− 16.5]	—		●	52[b] [− 1.4]	—		—		●	92 [− 0.17]	●	120 [− 4.4]	●

[a] Temperature of melting of the crystals on first heating. All temperatures in other columns relate to cooling cycles, and those in column 2 are recrystallization temperatures.

[b] Monotropic phases.

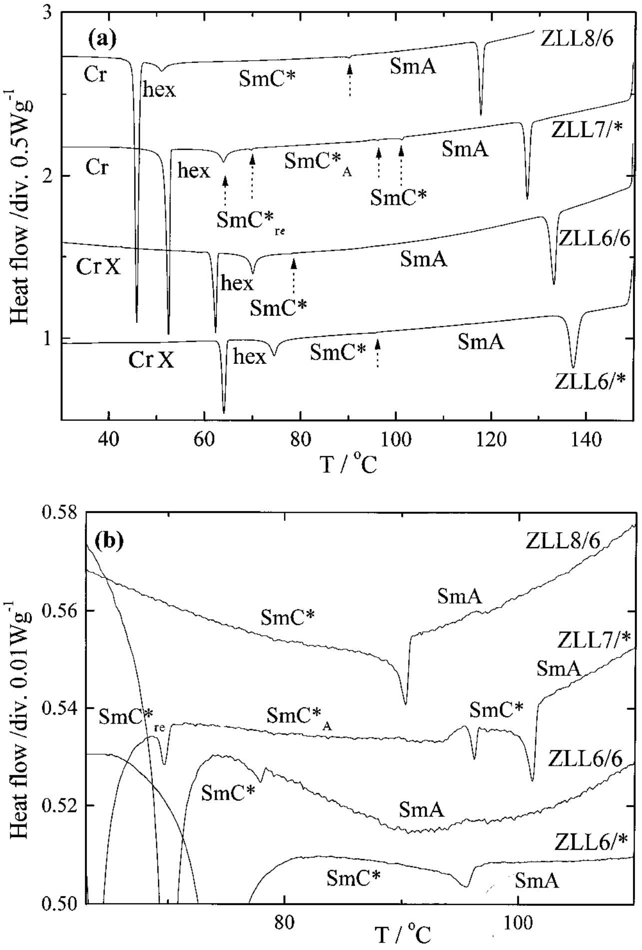

Figure 1. Typical DSC plots for the ZLL series measured on cooling. The arrows in (*a*) mark indistinct phase transitions, which are seen in enlarged view in (*b*). The slopes are adjusted for convenience. Compounds and phases are indicated.

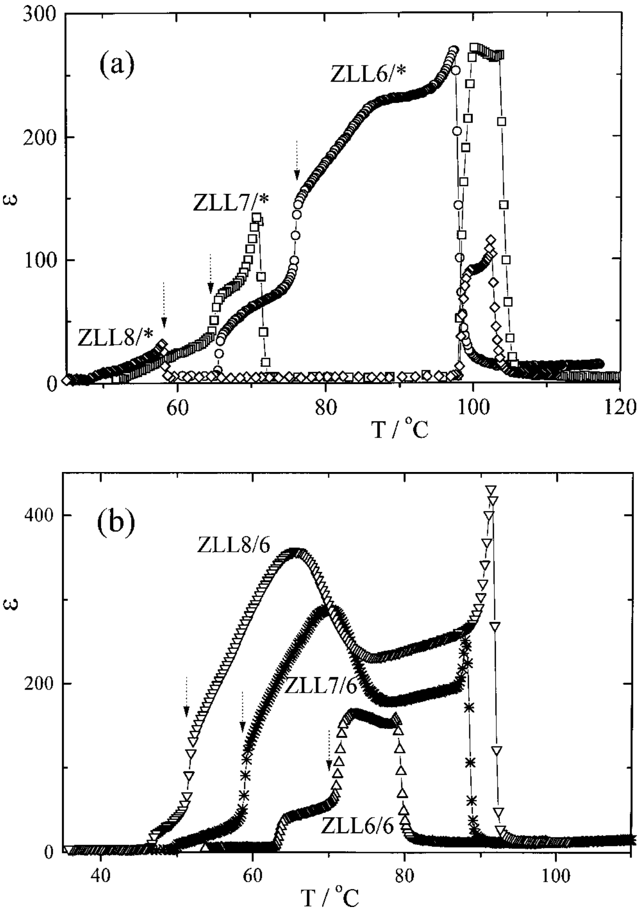

Figure 2. Temperature dependence of the real part of the permittivity measured at 30 Hz during cooling at a rate of 2 K min^{-1} for materials with (*a*) three and (*b*) two chiral centres. The arrows show the transition to the hexatic phase.

3.2. *Dielectric properties*

Low frequency permittivity was measured on cooling on aligned samples for all the compounds studied. Its real part, ε, is shown in figures 2(*a*) and 2(*b*) for homologues ZLL *n*/* and ZLL *n*/*m*, respectively. For all compounds, there is a significant increase in ε on reaching the SmC* phase on cooling. The maximum at the SmA–SmC* phase transition is caused by the contribution of the soft mode, which might be rather strong at this transition. The other maximum in the $\varepsilon(T)$ dependence in the SmC* phase that occurs in the ZLL *n*/*m* series, figure 2(*b*), does not correspond to any transition. It is connected with changes of the pitch length of the helicoidal structure [6] (details will be published separately).

In homologues ZLL7/* and ZLL8/* the SmC* phase is narrow and a fall of ε to very low values suggests the occurrence of the $\mathrm{SmC}^*_{\mathrm{A}}$ below the SmC* phase, see figure 2(*a*). Below the $\mathrm{SmC}^*_{\mathrm{A}}$ phase a further increase in ε is observed. In ZLL8/* it is connected with the occurrence of the hexatic phase (see also the next paragraph). The value of ε in the hexatic phase does not reach that detected in the SmC* phase, but it is nearly one order of magnitude higher compared with the values usually detected in AF hexatic phases [7]. For this reason we suggest that this phase is FE, either a SmI* or a SmF* phase. The transition from $\mathrm{SmC}^*_{\mathrm{A}}$ to FE SmI* phase has already been reported in [8]. In ZLL7/* the increase of ε below the $\mathrm{SmC}^*_{\mathrm{A}}$ phase, being a lot higher, represents the transition to the $\mathrm{SmC}^*_{\mathrm{re}}$ phase.

For other compounds studied, the hexatic phase also exists, but evolves directly from the SmC* phase. The SmC*–hexatic transition is manifested by a decrease in ε (see figure 2). In the low temperature CrX phase ε is still lower.

3.3. *X-ray studies*

X-ray studies have been performed on non-aligned samples. In figure 3, the smectic layer spacings, *d*, are shown as functions of temperature for ZLL7/*, ZLL8/* and ZLL6/6. This clearly shows a typical decrease of *d* at the onset of the tilted SmC* phase on cooling, which reflects the tilt of the molecules. With ZLL7/* and ZLL8/*, *d* continues to decrease within the $\mathrm{SmC}^*_{\mathrm{A}}$ phase. On approaching the next phase transition on cooling, *d* starts to increase and an inflection point in the increase represents the transition. In agreement with previous inferences, we conclude that for ZLL7/* and ZLL8/* this is the phase transition to the hexatic phase. Stretching of the aliphatic molecular chains and increased orientational order of the molecular long axes is the cause of the increase of *d* at the hexatic phase transition [9, 10]. Pre-transitional effects are a cause of the increase in *d* above the transition to the hexatic phase. In the hexatic phase *d* might be even higher than that in the non-tilted SmA phase. In ZLL7/*, the $\mathrm{SmC}^*_{\mathrm{re}}$ phase is inserted between the AF and hexatic phase, but is not clearly distinguished in the layer spacing data (see figure 3). On further cooling a more pronounced jump in the $d(T)$ dependence takes place owing to the occurrence of the low temperature CrX phase or crystal phase.

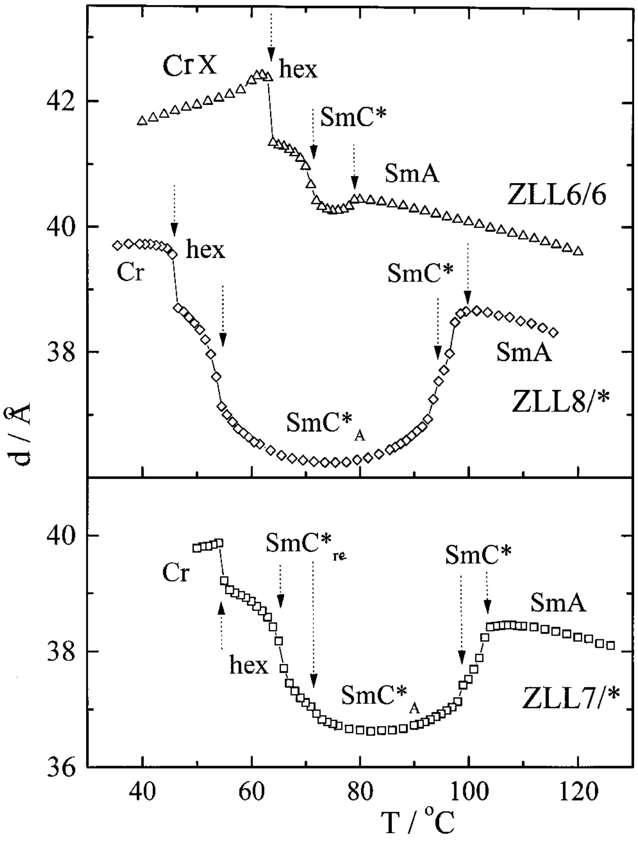

Figure 3. Temperature dependences of the layer spacing for the compounds indicated. Phases and phase transitions (arrows) are indicated.

3.4. *Spontaneous quantities and switching properties*

The spontaneous polarization, $\mathbf{P}_s$, and spontaneous tilt angle, θ_s, were measured in the FE, AF and hexatic phases. The values of $\mathbf{P}_s$ were determined from the $\mathbf{P}(\mathbf{E})$ hysteresis loop detected during $\mathbf{P}_s$ switching in an a.c. electric field. The θ_s values were calculated from the difference between the extinction positions observed in a planar sample between crossed polarizers under an opposing d.c. field high enough to unwind the helical structure. Well-aligned samples have to be used for θ_s measurements.

The temperature dependences of $\mathbf{P}_s$ and θ_s are shown in figures 4(*a*) and 4(*b*), respectively. The values of $\mathbf{P}_s$ increase on cooling within the SmC* and $\mathrm{SmC}^*_{\mathrm{A}}$ phases

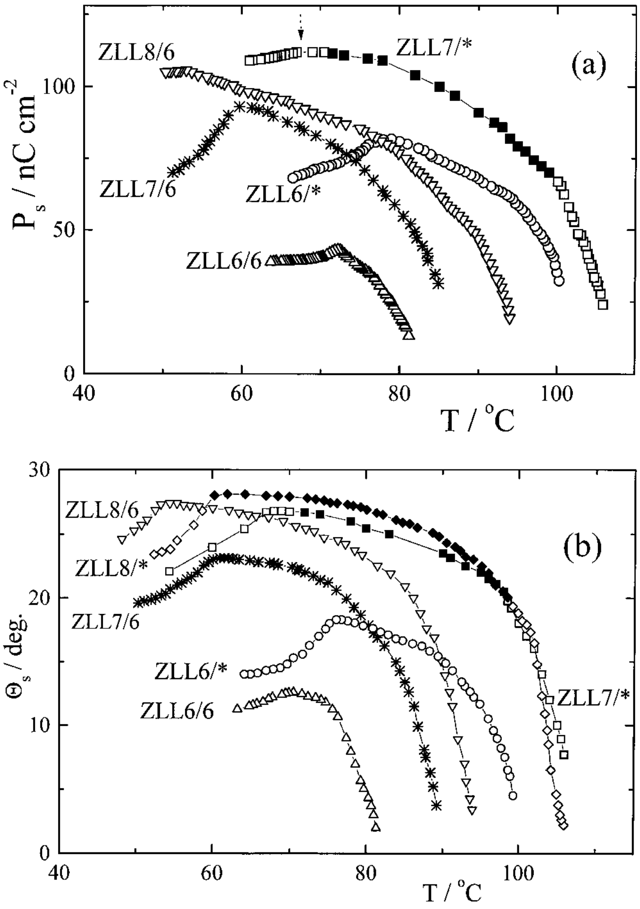

Figure 4. Temperature dependences of (*a*) spontaneous polarization and (*b*) spontaneous tilt angle for the materials indicated. The decrease in the values with falling temperature corresponds to the transition to the hexatic phase. The full symbols indicate the $\mathrm{SmC}^*_{\mathrm{A}}$ phase; the arrow in (*a*) indicates the transition to the $\mathrm{SmC}^*_{\mathrm{re}}$ phase.

without any anomaly at the phase transition between them. At the transition to the hexatic phase a decrease of $\mathbf{P}_s$ values occurs, which is very sharp for ZLL7/6, ZLL6/6, and ZLL6/*, see figure 4 (*a*). In ZLL7/* a slight decrease is detected even in the $\mathrm{SmC}^*_{\mathrm{re}}$ phase. A significant decrease in the θ_s values occurs on reaching the hexatic phase for all the compounds studied. Let us point out that in [11], the same behaviour of $\mathbf{P}_s$ at the SmC*–SmI* phase transition was found. On the other hand, for other FE and AF materials, an increase in the $\mathbf{P}_s$ values and no anomaly in the θ_s values have been observed at the transition to the hexatic phase [7, 12].

As far as the coercive field detected from the hysteresis loops is concerned, it becomes slightly higher in the AF phase than in the FE phase, but increases sharply in the hexatic phase. When approaching the lower limit of this phase, switching becomes impossible, as is the case in the low temperature crystalline phase.

It is possible to distinguish between the FE and AF SmC phases by measuring the d.c. threshold electric field E_{th}. It is rather high in the AF phase, but critically decreases to zero when approaching the FE phase. In the AF phase of ZLL8/* $E_{\mathrm{th}} = 5\ \mathrm{V}\ \mu\mathrm{m}^{-1}$, and for ZLL7/* $E_{\mathrm{th}} = 2.5\ \mathrm{V}\ \mu\mathrm{m}^{-1}$ and decreases to zero even at the low temperature limit of the AF phase. This confirms the existence of the $\mathrm{SmC}^*_{\mathrm{re}}$ phase below the AF phase in the ZLL7/* homologue.

4. Discussion and conclusions

The ZLL compounds studied can be compared with a series denoted M2 studied in [2]. These series differ in the linkage between the core and the chiral part, which is an ester group for ZLL and an ether linkage for M2. In the ZLL series, one chiral centre more had to be introduced into the chiral chain to obtain the AF phase. However, this AF phase was stable compared with the monotropic one in the M2 series. In the ZLL *n*/*m* series with two chiral centres only, the AF phase was lost. The disappearance of the $\mathrm{SmC}^*_{\mathrm{A}}$ in this series might result from the identical configuration of the two chiral centres in the molecule. It is difficult to infer whether the occurrence of the AF phase is mainly connected with the type of linkage in the vicinity of the mesogenic core, or if the configuration of the chiral centres is more important. The ramification of the end of the chiral chain does not seem to be essential for the existence of the AF phase, and recently, we have synthesized a new, similar homologous series with the same non-ramified chain as in ZLL *n*/*m*, which also exhibits the AF phase.

The hexatic phase, which occurs in all the compounds studied in the ZLL series, was not observed in the M2 series. To achieve the hexatic phase, the M2 structure has to be modified by introducing a double bond at the end of the alkyl chain.

The hexatic phases (either SmI or SmF) were not definitely characterized. X-ray studies on oriented samples are necessary to establish the structure. However, one can suppose that they are ferroelectric in all cases, because the upper phase is also FE, except for ZLL8/*. In ZLL8/* however, the hexatic phase is probably also FE, despite the preceding phase being AF ($\mathrm{SmC}^*_{\mathrm{A}}$). The indication is the high permittivity detected in this hexatic phase. A detailed study of these hexatic phases is being carried out.

Theory describing the dielectric properties around the phase transition to the hexatic (either FE or AF) phase [7, 12] requires that the spontaneous tilt angle θ_s is saturated, i.e. it should exhibit no changes at the phase transition to the hexatic phase. For this reason existing theory cannot be directly applied to the compounds studied here which exhibit anomalies at this transition. A modification of the theory will be proposed in a further paper, together with a detailed dielectric study.

The existence of either SmC* or $\mathrm{SmC}^*_{\mathrm{A}}$ phases is driven by interlayer interactions which reflect a competition between molecular interlayer penetration (preferring FE order) and attractive van der Waals interactions (preferring AF order) [13]. The occurrence of a re-entrant SmC* phase below the $\mathrm{SmC}^*_{\mathrm{A}}$ phase was reported first and plausibly explained in [14]. The driving force for this phenomenon has been established as increasing quadrupolar ordering when the temperature is decreased. This effect facilitates the interlayer molecular penetration and in this way promotes the reappearance of the SmC* phase at lower temperatures [14].

The authors wish to acknowledge discussions with E. Gorecka on the re-entrant ferroelectric phase. This work was supported by grant No. 202/99/1120 from the Grant Agency of the Czech Republic and KBN grant 3T09A 046 15.

References

[1] Taniguchi, H., Ozaki, M., Yoshino, K., Satoh, K., and Yamasaki, N., 1998, *Ferroelectrics*, **77,** 137.

[2] Mery, S., Lötzsch, D., Heppke, G., and Shashidhar, R., 1997, *Liq. Cryst.*, **23,** 629.

[3] Johnson, W. S., Butsche, C. D., and Offenhauer, R. D., 1946-7, *J. Am. chem. Soc.*, **68,** 1648.

[4] Kašpar, M., Hamplovà, V., Pakhomov, S. A., Bubnov, A. M., Guittard, F., Sverenyàk, H., Stibor, I., and Vaněk, P., 1998, *Liq. Cryst.*, **24,** 599.

[5] Pyzuk, W., Gòrecka, E., Szydłowska, J., Krowczynski, A., and Pociecha, D., 1995, *Phys. Rev. E*, **52,** 1748.

[6] Bourny, V., Pavel, J., Gisse, P., and Nguyen, H. T., 2000, *Ferroelectrics*, **241,** 247.

[7] Glogarovà, M., Pociecha, D., Gòrecka, E., Rychetskỳ I., and Mieczkowski, J., 2000, *Ferroelectrics*, **245,** 715.

[8] Neudorf, M., Takanishi, Y., Fukuda, A., Saito, S., Murashiro, K., Inukai, T., and Demus, D., 1995, *J. mater. Chem.*, **5,** 2221.

[9] Krishna Prasad, S., Shankar Rao, D. S., Chandrasekhar, S., Neubert, M. E., and Goodby, J. W., 1995, *Phys. Rev. Lett.*, **74,** 270.

[10] Szydłowska, J., Pociecha, D., Gòrecka, E., Kardas̀, D., Mieczkowski, J., and Przedmojski, J., 1999, *J. mater. Chem.*, **9,** 361.

[11] Krishna Prasad, S., Nair, G. G., and Chandrasekhar, S., 1995, *J. mater. Chem.*, **5,** 2253.

[12] Rychetskỳ, I., Pociecha, D., Dvořàk, V., Mieczkowski, J., and Glogarovà, M., 1999, *J. chem. Phys.*, **111,** 1541.

[13] Škarabot, M., Čepič, M., Žekš, B., Blinc, R., Heppke, G., Kityk, A. V., and Muševič, I., 1998, *Phys. Rev. E*, **58,** 575.

[14] Pociecha, D., Gòrecka, E., Čepič, M., Vaupotič, N., Žekš, B., Kardas̀, D., and Mieczkowski, J., 2001, *Phys. Rev. Lett.*, **86,** 3048.